

LETTER TO THE EDITOR

On the Sensitivity of Halo Shape Measurements

Moritz S. Fischer^{1,2,3} and Lucas M. Valenzuela¹

¹ Universitäts-Sternwarte, Fakultät für Physik, Ludwig-Maximilians-Universität München, Scheinerstr. 1, D-81679 München, Germany

e-mail: mfisher@usm.uni-muenchen.de

² Excellence Cluster ORIGINS, Boltzmannstrasse 2, D-85748 Garching, Germany

³ Hamburger Sternwarte, Universität Hamburg, Gojenbergsweg 112, D-21029 Hamburg, Germany

Received XX Month, 20XX / Accepted XX Month, 20XX

ABSTRACT

Shape measurements of galaxies and galaxy clusters are widespread in the analysis of cosmological simulations. But the limitations of those measurements have been poorly investigated. In this paper, we explain why the quality of the shape measurement does not only depend on the numerical resolution, but also on the density gradient. In particular, this can limit the quality of measurements in the central regions of haloes. We propose a criterion to estimate the sensitivity of the measured shapes based on the density gradient of the halo and apply it to cosmological simulations of collisionless and self-interacting dark matter. By this, we demonstrate where reliable measurements of the halo shape are possible and how cored density profiles limit their applicability.

Key words. methods: numerical – methods: data analysis – galaxies: general

1. Introduction

The shapes of galaxies and more massive objects like galaxy clusters have been measured in numerous publications. In simulations, it is simple to measure the shape of various components like stars, gas, or dark matter (DM).

The shape of astrophysical objects is of interest because it can be affected by various physical mechanisms and thus measurements of the shape potentially allow us to learn about such processes. For instance, Chua et al. (2022) studied the impact of galactic feedback on the shape of dark matter haloes. They also gained interest in studies of dark matter, for example, self-interacting dark matter (SIDM) tends on average to make haloes more round (e.g. Peter et al. 2013).

Shapes have been measured in N -body simulations for a long time, starting with early DM-only simulations (e.g. Katz 1991) and the first larger cosmological simulations (e.g. Springel et al. 2004; Allgood et al. 2006; Bett et al. 2007) to study the DM halo shapes and their relations to other properties, such as mass and spin. Such studies found that DM haloes are generally prolate, that is elongated in shape. More recent work has been done on using hydrodynamical cosmological simulations to study the impact of baryons and the cosmic web environment on shapes (e.g. Zemp et al. 2012; Bryan et al. 2013; Chua et al. 2019; Cataldi et al. 2021; Hellwing et al. 2021). Also, the stellar component and its shape in hydrodynamical simulations have been studied in recent years (e.g. Pulsoni et al. 2020; Emami et al. 2021b; Valenzuela et al. in prep.).

There exist a variety of methods to infer the shapes from N -body simulations. A number of these methods have been studied and compared by Zemp et al. (2011), and additional methods have also been applied in other works (e.g. Warnick et al. 2008; Emami et al. 2021a). However, the limitations of the sensitivity of the shape measurements, and with this their accuracy, have been poorly studied. Typically, one has only used lower thresholds for

the number of particles that should be included in the ellipsoidal shell used to determine the shape. For example, Zemp et al. (2011) recommended requiring at least a few thousand particles to lie within each shell. Other authors have also set lower thresholds of 1000 particles per shell (e.g. Pulsoni et al. 2020). In this letter, we point out that a large number of particles is not sufficient to measure accurate shapes, but that the density gradient matters, too.

Given a constant density, it is unclear what its shape is. In this particular case, it is not defined and thus cannot be measured. It is known that haloes can have density cores, that is, their central density is roughly constant. Mechanisms that can reduce the central density to be constant include supernova feedback and DM self-interactions. Given such a density core, state-of-the-art algorithms can nevertheless return a shape, though it is anything but reliable. Here, the discretisation noise of the N -body simulations starts to play a crucial role. If it is larger than the density gradient, it may dominate the shape measurement and the obtained shape can be far off from the physical shape. In this case, it would typically return shapes that are too elliptical. To understand this quantitatively, we develop a criterion to measure how accurate the inferred shapes are.

Such a criterion is of interest for any studies that rely on the measurement of shapes, for example in the context of DM (e.g. Despali et al. 2022; Shen et al. 2022) or the impact of baryons (e.g. Springel et al. 2004; Prada et al. 2019).

In this section, we have described the problem at hand. The following section (Sect. 2) deals with how we measure shapes and we introduce the criterion to estimate the sensitivity of the shape measurement. In Sect. 3, we measure the shape of simulated haloes and study the effect of density cores. Subsequently, in Sect. 4, we discuss our findings. Finally, we conclude in Sect. 5.

2. Shapes

In this section, we describe how we measure shapes, derive the criterion for the shape sensitivity and discuss the role of the convergence criterion.

2.1. Measuring shapes

In the literature various methods have been applied to measure shapes (e.g. Allgood et al. 2006; Bett et al. 2007; Warnick et al. 2008; Zemp et al. 2011; Bett 2012; Schneider et al. 2012; Peter et al. 2013; Robertson et al. 2019; Banerjee et al. 2020; Chua et al. 2021; Sameie et al. 2018; Fischer et al. 2021b; Harvey et al. 2021; Varga et al. 2022). For this work we use an iterative procedure where we select particles in a given volume and infer their shape from the mass tensor:

$$\mathbf{M}_{ij} = \sum_k m_k r_{k,i} r_{k,j} \quad (1)$$

Here, k denotes a particle and i, j are the coordinate indices. The axis ratios follow from the eigenvalues ($\lambda_1 \geq \lambda_2 \geq \lambda_3$): $q = \sqrt{\lambda_2/\lambda_1}$ and $s = \sqrt{\lambda_3/\lambda_1}$. We use them to compute the new shape of the selection volume and the eigenvectors to compute its orientation. The mass tensor is again computed from the particles in the new selection volume. We continue this procedure until the axis ratios of the selection volume converge against the one calculated from the mass tensor.

In this letter we use two methods: we select particles within ellipsoids and ellipsoidal shells (homoeoids). The volume of an ellipsoid is given by $V = 4/3\pi a b c$, with the semi-axes $a \geq b \geq c$. The radius that corresponds to the same volume of a sphere is $r^3 = a b c$. Their ratios are $q = b/a$ and $s = c/a$. To select the particles within a volume we introduce

$$\tilde{r}_{\text{ell}}^2 := x^2 (q s)^{2/3} + y^2 q^{-4/3} s^{2/3} + z^2 q^{2/3} s^{-4/3}, \quad (2)$$

which ensures that the volume of the ellipsoids remains constant. Here, x, y , and z denote the spatial coordinates. If \tilde{r}_{ell}^2 is smaller than r , the particles are selected for the ellipsoids. In the case of the ellipsoidal shells, there also exists a lower limit on \tilde{r}_{ell}^2 . In practice, we use the same implementation as previously used in Fischer et al. (2022).

2.2. Criterion for the shape sensitivity

The density gradients are important for the sensitivity of the shape measurement. If they are low, the discretisation error may dominate and the shape can no longer be calculated reliably. In the case of measuring the shape within ellipsoidal shells, one can calculate the sensitivity as follows. The discretisation noise can be estimated as $\sqrt{N_i}$, where N_i is the number of particles in a shell i . Hence, the relative error is $N_i^{-1/2}$. Given the number density of the shell, n_i , its error is then $n_i N_i^{-1/2}$. We can relate this to the density gradient by simply computing the finite difference in the number density of the neighbouring shells. Thus, a condition for the shape measurement to be sensitive can be found as:

$$|n_{i-1} - n_{i+1}| > n_i N_i^{-1/2}. \quad (3)$$

From this, we derive ξ as a measure of the sensitivity, which should be larger than unity:

$$\xi_i \equiv \frac{V_i}{\sqrt{N_i}} \left| \frac{N_{i-1}}{V_{i-1}} - \frac{N_{i+1}}{V_{i+1}} \right| > 1. \quad (4)$$

V_i denotes the volume of shell i , with $n_i = N_i/V_i$. Alternatively one may express the condition as

$$\Delta x_i \left| \frac{dn}{dx} \right|_i > n_i N_i^{-1/2}, \quad (5)$$

where Δx_i denotes the thickness of the shell.

When not using shells, but all particles included in an ellipsoid, a similar criterion can be obtained by introducing a parameter $\gamma = r_2/r_1$ that defines the relative thickness of a shell, with $r_1 > r_2$ being the radius of the ellipsoid and the inner shell radius, respectively. The thickness Δx_i from Eq. 5 then is found to be $\Delta x_i = x_i(1 - \gamma)$, with the ellipsoid radius x_i . The idea is that the particles within Δx_i are the main contributors to the mass tensor and thus can be used to estimate the discretisation noise. Now we can rewrite the condition as,

$$\xi_i \equiv \sqrt{\frac{4\pi}{3n_i}} \left| \frac{dn}{dx} \right|_i x_i^{5/2} \alpha > 1. \quad (6)$$

For this, we introduced $\alpha := (1 - \gamma)\sqrt{1 - \gamma^3}$ and assume it to be constant¹. In the following we use $\alpha = 0.5$.

According to the derivation above, $\xi > 1$ is required only. However, in practice we recommend using a more stringent criterion, for example, $\xi > 10$, to include a safety margin. We found a value of 1 to be too low; instead, a value of 10 is motivated by our findings in Sect. 3 and Appendix A.

2.3. Convergence criterion

The convergence criterion plays a major role. If the typical fluctuations in the axis ratios arising from the discrete nature of the N -body representation are larger than the convergence criterion, the shapes can become more and more elliptical with each iteration. To solve this problem, the convergence criterion could be chosen less strict such that it is larger than the discretisation noise. However, this would come at the cost of being biased towards the initial chosen shape, typically a sphere. We do not follow this approach but choose a strict convergence criterion in the following and require that the inferred axis ratios do not vary by more than 0.1% per iteration. If we do not converge within 50 iterations we stop and take the last shape found. In practice, this occurs only if a small number of particles is used for the tensor calculation and thus affects the shape at small radii only.

3. Simulated haloes

In this section, we measure the shape of simulated DM haloes and investigate their accuracy. We use the four most massive haloes of the full box cosmological simulations presented in Fischer et al. (2022). The same analysis to identify substructure and compute corresponding quantities such as the halo mass and the virial radius is employed, that is, we use SUBFIND (Springel et al. 2001; Dolag et al. 2009). Moreover, we use the simulations with the highest resolution ($N = 576^3$, $m_{\text{DM}} = 4.37 \times 10^7 M_\odot h^{-1}$) for collisionless cold dark matter (CDM) and frequently self-interacting dark matter (fSIDM) with a momentum transfer cross-section of $\sigma_{\bar{T}}/m = 0.1 \text{ cm}^2 \text{ g}^{-1}$ (Kahlhoefer et al. 2014; Fischer et al. 2021a). For further details see Fischer et al. (2022).

¹ Strictly speaking, α depends on the density gradient. For steep gradients, it would be larger than for flat ones as in the first case a larger contribution to the mass tensor stems from smaller radii. Nevertheless, we set α to a constant value to simplify the calculations.

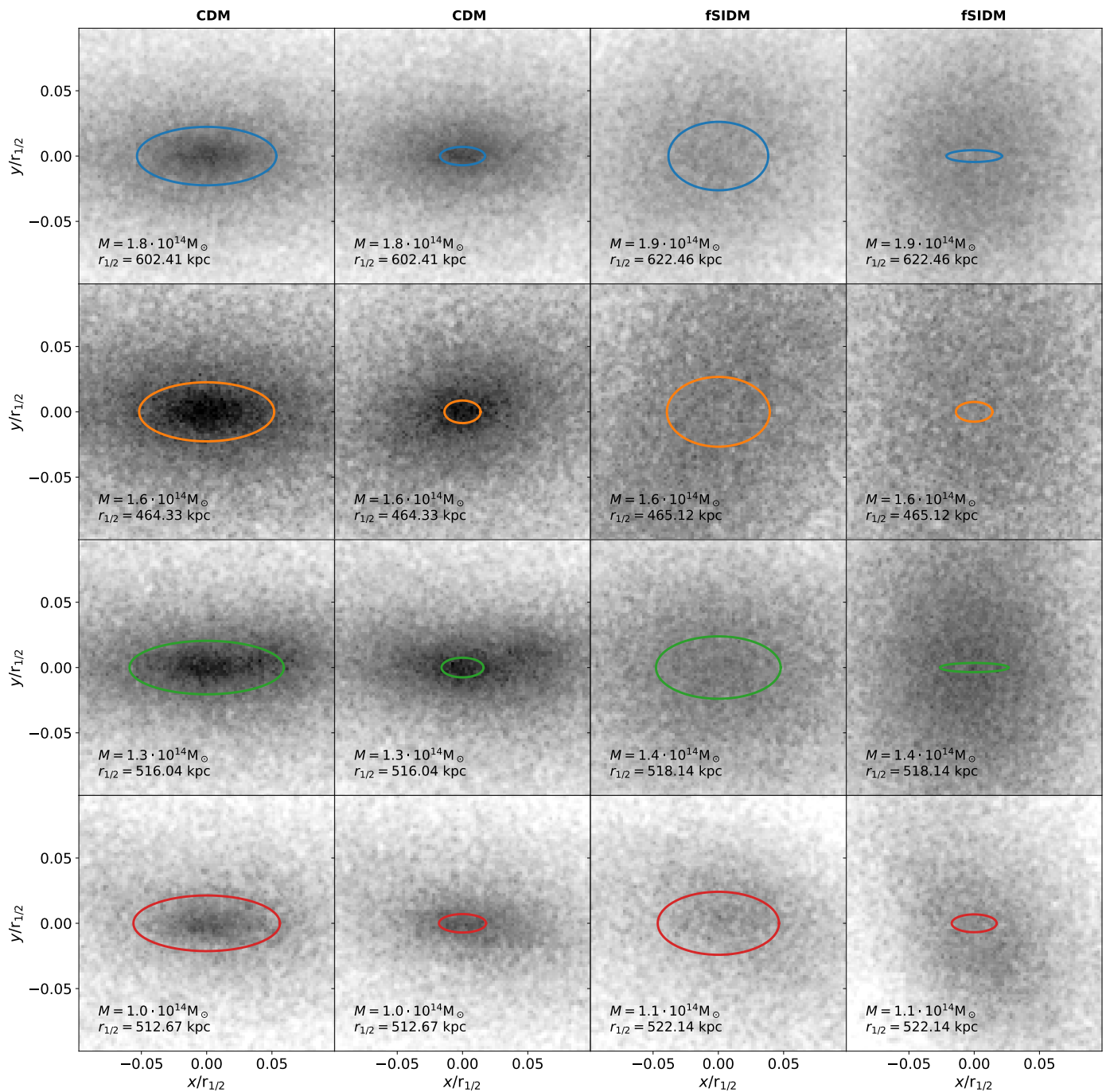


Fig. 1. The DM surface density is shown for the primary subhaloes simulated with CDM (the two left columns) and fSIDM with $\sigma_{\bar{T}}/m = 0.1 \text{ cm}^2 \text{ g}^{-1}$ (the two right columns). We note that the colour scaling is logarithmic. The shapes are measured within a volume of $V = 4/3 \pi (0.032 r_{1/2})^3$ (odd columns) and $V = 4/3 \pi (0.0105 r_{1/2})^3$ (even columns). They are illustrated with coloured ellipses. The haloes are shown face-on according to the measured shapes. We matched the haloes across the simulation, where matched haloes are shown in the same row and the same colour is used for the ellipses.

In Fig. 1 we show the DM surface density in the central region of the four most massive haloes. Only the particles belonging to the primary subhalo as identified by SUBFIND are used, by this we avoid including satellite substructure. We have measured the shape within a volume of $V = 4/3 \pi (0.032 r_{1/2})^3$ and $V = 4/3 \pi (0.0105 r_{1/2})^3$, indicated by the coloured ellipses. The primary subhaloes are aligned according to this shape measurement and are shown face-on. We find that the CDM haloes (left-hand side) are more elliptical than the fSIDM haloes (right-

hand side). By eye, the inferred shapes seem to roughly match the underlying DM distribution for the odd columns. This is in contrast to the even columns where we do the same, but measure the shape at smaller distances to the centre. For the CDM haloes (left-hand side) they seem to agree with the surface density plots, but do not match for fSIDM haloes (right-hand side). For the latter case, the volume used for the shape measurement lies within the density core formed due to the DM self-interactions. The van-

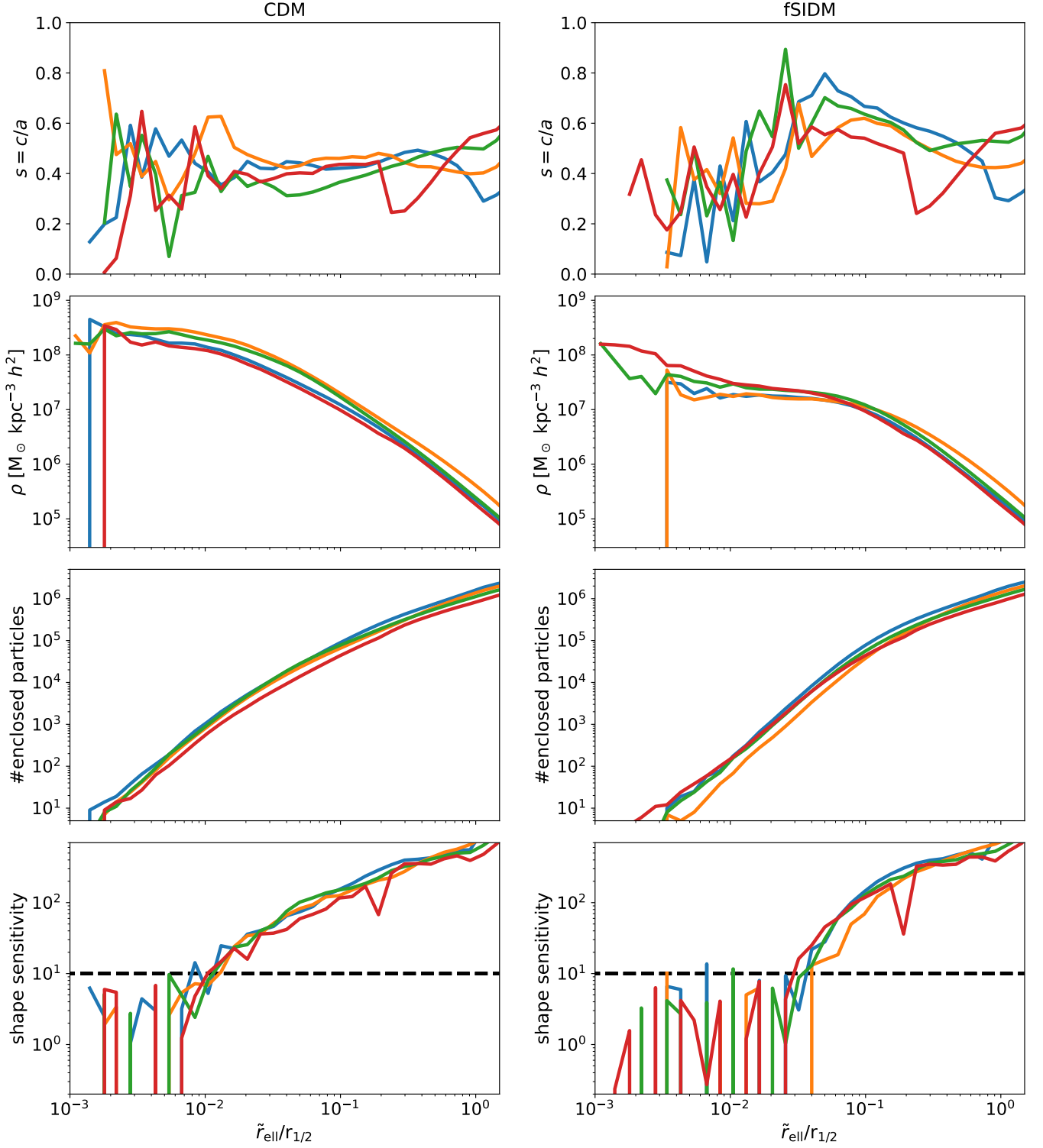


Fig. 2. Various quantities for the CDM (right-hand side) and fSIDM (left-hand side) haloes (same as in Fig. 1, colours are the same) are shown as a function of \tilde{r}_{ell} . First row: The shape profile as the ratio of the major and minor axis is shown. The mass tensor is measured within ellipsoids. Second row: The density profile is shown as inferred from the ellipsoids used for the shape measurement by taking the differences in mass and volume between two consecutive ellipsoids. Third row: The number of particles enclosed in the ellipsoid is shown. Fourth row: The shape sensitivity, ξ , is shown according to Eq. 6. Here the vertical line indicates the criterion above which the shape is measured accurately, $\xi = 10$.

ishing density gradient causes trouble in identifying the shape as we would expect from Sect. 2.

In Fig. 2 we show the shape and the density profiles as well as the number of particles enclosed within the ellipsoids and

the shape sensitivity as a function of \tilde{r}_{ell} . In Appendix A we have carried out the same analysis, but measure the shapes in shells. We can clearly see that the density core present in the fSIDM haloes (right-hand side) affects the accuracy at which the

shapes can be measured compared to CDM (left-hand side). At small distances, the inferred shape from the fSIDM haloes (upper panel right-hand side) can be even more elliptical than the CDM one (upper panel left-hand side). This is non-physical and an artefact arising from the low shape sensitivity. It is insufficient to explain this by a lower number of enclosed particles as the shape measure becomes unreliable at particle numbers for which the CDM shapes are still reasonable. For both the ellipsoid and the ellipsoidal shell method, a shape sensitivity of $\xi \geq 10$ is found to be a good criterion for obtaining robust shape measurements, as can be seen from the top and bottom rows of Figs. 2 and A.1.

We note that it can also be the case that at large radii the shape cannot be measured accurately. This could be due to substructure, an example would be the halo indicated in red. As we only select particles that belong to the primary subhalo, this effect is however suppressed.

4. Discussion

In this section, we discuss the implications of our results regarding the sensitivity of halo shape measurements.

In cosmological simulations often a convergence radius according to Power et al. (2003) is computed. Stadel et al. (2009) noticed that the convergence radius for the shape in DM-only simulations of CDM is roughly three times larger than the one of the density profile. We found that additional physical processes can break the idea that the shape could be safely determined beyond a certain radius defined by the numerical resolution.

In contrast, the accuracy of measured shapes does not purely depend on the numerical properties, but also on the underlying physical matter distribution. Implying that a different criterion, such as the one derived in Sect. 2.2, is needed, taking the density gradient into account.

It is crucial to be aware of this when comparing simulation results to observations. For example, the deprojection algorithm of de Nicola et al. (2020) allows inferring shapes of observed galaxies and can be used for comparison (de Nicola et al. 2022). But results have to be taken with caution if the accuracy of the simulated shapes is unclear. This is even true for pure theoretical studies that for example investigate the impact of feedback on the halo shape (e.g. Chua et al. 2022). An approach different from computing 3D shapes would be to create mock observations from the simulation data and use them for comparison as done by Harvey et al. (2020).

We found that density cores are prohibitive for reliable shape measurements. The ones we studied were formed by DM self-interactions, but also other mechanisms such as baryonic processes, for example, supernovae (e.g. Read & Gilmore 2005) or black hole feedback (e.g. Martizzi et al. 2013), can reduce the density gradient in the halo centre. Whenever a density core is present, it undermines the ability to measure meaningful shapes.

Depending on the density profile, shapes cannot be measured at arbitrarily small radii. Increasing the resolution of the simulation will hardly improve the situation if density cores continue to be present. Instead, we suggest measuring shapes only beyond the radius of the density core and verifying their reliability with our shape sensitivity criterion.

5. Conclusion

In this letter, we have introduced a criterion to estimate the sensitivity of shape measurements from N -body simulation data and measured the shapes of various haloes to verify the criterion. Our main conclusions are:

- The accuracy of measured shapes does not only depend on the numerical resolution but also on the density gradient.
- Density cores lead to problematic measurements of shapes in the central region of haloes.
- Care must be taken about the quality of measured shapes, which can be inferred from the criterion in Eq. 4 (Eq. 6) when the shape is measured employing a mass tensor computed from particles in elliptical shells (ellipsoids).

Future studies can improve the reliability of their measured shapes by employing the presented shape sensitivity criterion to ensure determining physically meaningful shapes.

Acknowledgements. We thank Marcus Brüggen and Klaus Dolag for comments and Stefano de Nicola, Roberto P. Saglia and Jens Thomas for inspiring discussion. LMV acknowledges support by the COMPLEX project from the European Research Council (ERC) under the European Union’s Horizon 2020 research and innovation program grant agreement ERC-2019-AdG 882679. This work is funded by the Deutsche Forschungsgemeinschaft (DFG, German Research Foundation) under Germany’s Excellence Strategy – EXC 2121 “Quantum Universe” – 390833306, Germany’s Excellence Strategy – EXC-2094 “Origins” – 390783311. Software: NumPy (Harris et al. 2020), Matplotlib (Hunter 2007).

References

- Allgood, B., Flores, R. A., Primack, J. R., et al. 2006, MNRAS, 367, 1781
 Banerjee, A., Adhikari, S., Dalal, N., More, S., & Kravtsov, A. 2020, J. Cosmology Astropart. Phys., 2020, 024
 Bett, P. 2012, MNRAS, 420, 3303
 Bett, P., Eke, V., Frenk, C. S., et al. 2007, MNRAS, 376, 215
 Bryan, S. E., Kay, S. T., Duffy, A. R., et al. 2013, Monthly Notices of the Royal Astronomical Society, 429, 3316
 Cataldi, P., Pedrosa, S. E., Tissera, P. B., & Artale, M. C. 2021, MNRAS, 501, 5679
 Chua, K. T. E., Dibert, K., Vogelsberger, M., & Zavala, J. 2021, MNRAS, 500, 1531
 Chua, K. T. E., Pillepich, A., Vogelsberger, M., & Hernquist, L. 2019, MNRAS, 484, 476
 Chua, K. T. E., Vogelsberger, M., Pillepich, A., & Hernquist, L. 2022, MNRAS, 515, 2681
 de Nicola, S., Saglia, R. P., Thomas, J., et al. 2022, ApJ, 933, 215
 Despali, G., Walls, L. G., Vegetti, S., et al. 2022, arXiv e-prints [arXiv:2204.12502]
 de Nicola, S., Saglia, R. P., Thomas, J., Dehnen, W., & Bender, R. 2020, MNRAS, 496, 3076
 Dolag, K., Borgani, S., Murante, G., & Springel, V. 2009, Monthly Notices of the Royal Astronomical Society, 399, 497
 Emami, R., Genel, S., Hernquist, L., et al. 2021a, ApJ, 913, 36
 Emami, R., Hernquist, L., Alcock, C., et al. 2021b, ApJ, 918, 7
 Fischer, M. S., Brüggen, M., Schmidt-Hoberg, K., et al. 2021a, MNRAS, 505, 851
 Fischer, M. S., Brüggen, M., Schmidt-Hoberg, K., et al. 2022, MNRAS, 516, 1923
 Fischer, M. S., Brüggen, M., Schmidt-Hoberg, K., et al. 2021b, Monthly Notices of the Royal Astronomical Society, 510, 4080
 Harris, C. R., Millman, K. J., van der Walt, S. J., et al. 2020, Nature, 585, 357
 Harvey, D., Chisari, N. E., Robertson, A., & McCarthy, I. G. 2021, MNRAS, 506, 441–451
 Harvey, D., Robertson, A., Tam, S.-I., et al. 2020, MNRAS, 500, 2627
 Hellwing, W. A., Cautun, M., van de Weygaert, R., & Jones, B. T. 2021, Phys. Rev. D, 103, 063517
 Hunter, J. D. 2007, Computing in Science Engineering, 9, 90
 Kahlhoefer, F., Schmidt-Hoberg, K., Frandsen, M. T., & Sarkar, S. 2014, MNRAS, 437, 2865
 Katz, N. 1991, ApJ, 368, 325
 Martizzi, D., Teyssier, R., & Moore, B. 2013, MNRAS, 432, 1947
 Peter, A. H. G., Rocha, M., Bullock, J. S., & Kaplinghat, M. 2013, MNRAS, 430, 105
 Power, C., Navarro, J. F., Jenkins, A., et al. 2003, MNRAS, 338, 14
 Prada, J., Forero-Romero, J. E., Grand, R. J. J., Pakmor, R., & Springel, V. 2019, MNRAS, 490, 4877
 Pulsoni, C., Gerhard, O., Arnaboldi, M., et al. 2020, A&A, 641, A60
 Read, J. I. & Gilmore, G. 2005, MNRAS, 356, 107
 Robertson, A., Harvey, D., Massey, R., et al. 2019, MNRAS, 488, 3646–3662
 Sameie, O., Creasey, P., Yu, H.-B., et al. 2018, MNRAS, 479, 359

- Schneider, M. D., Frenk, C. S., & Cole, S. 2012, *J. Cosmology Astropart. Phys.*, 2012, 030
- Shen, X., Brinckmann, T., Rapetti, D., et al. 2022, arXiv e-prints [arXiv:2202.00038]
- Springel, V., White, S. D. M., & Hernquist, L. 2004, in *Dark Matter in Galaxies*, ed. S. Ryder, D. Pisano, M. Walker, & K. Freeman, Vol. 220, 421
- Springel, V., White, S. D. M., Tormen, G., & Kauffmann, G. 2001, *Monthly Notices of the Royal Astronomical Society*, 328, 726
- Stadel, J., Potter, D., Moore, B., et al. 2009, *Monthly Notices of the Royal Astronomical Society: Letters*, 398, L21
- Valenzuela, L. M., Remus, R.-S., & Dolag, K. in prep., arXiv e-prints
- Vargya, D., Sanderson, R., Sameie, O., et al. 2022, *MNRAS*
- Warnick, K., Knebe, A., & Power, C. 2008, *MNRAS*, 385, 1859
- Zemp, M., Gnedin, O. Y., Gnedin, N. Y., & Kravtsov, A. V. 2011, *The Astrophysical Journal Supplement Series*, 197, 30
- Zemp, M., Gnedin, O. Y., Gnedin, N. Y., & Kravtsov, A. V. 2012, *The Astrophysical Journal*, 748, 54

Appendix A: Shape measured in shells

For this appendix, we computed the shapes based on particles within shells. Consequently we use Eq. 4 to compute the shape sensitivity. Analogously to Fig. 2 we display the measured shapes and their sensitivity in Fig. A.1. Qualitatively we find the same as before for the particles enclosed in ellipsoids.

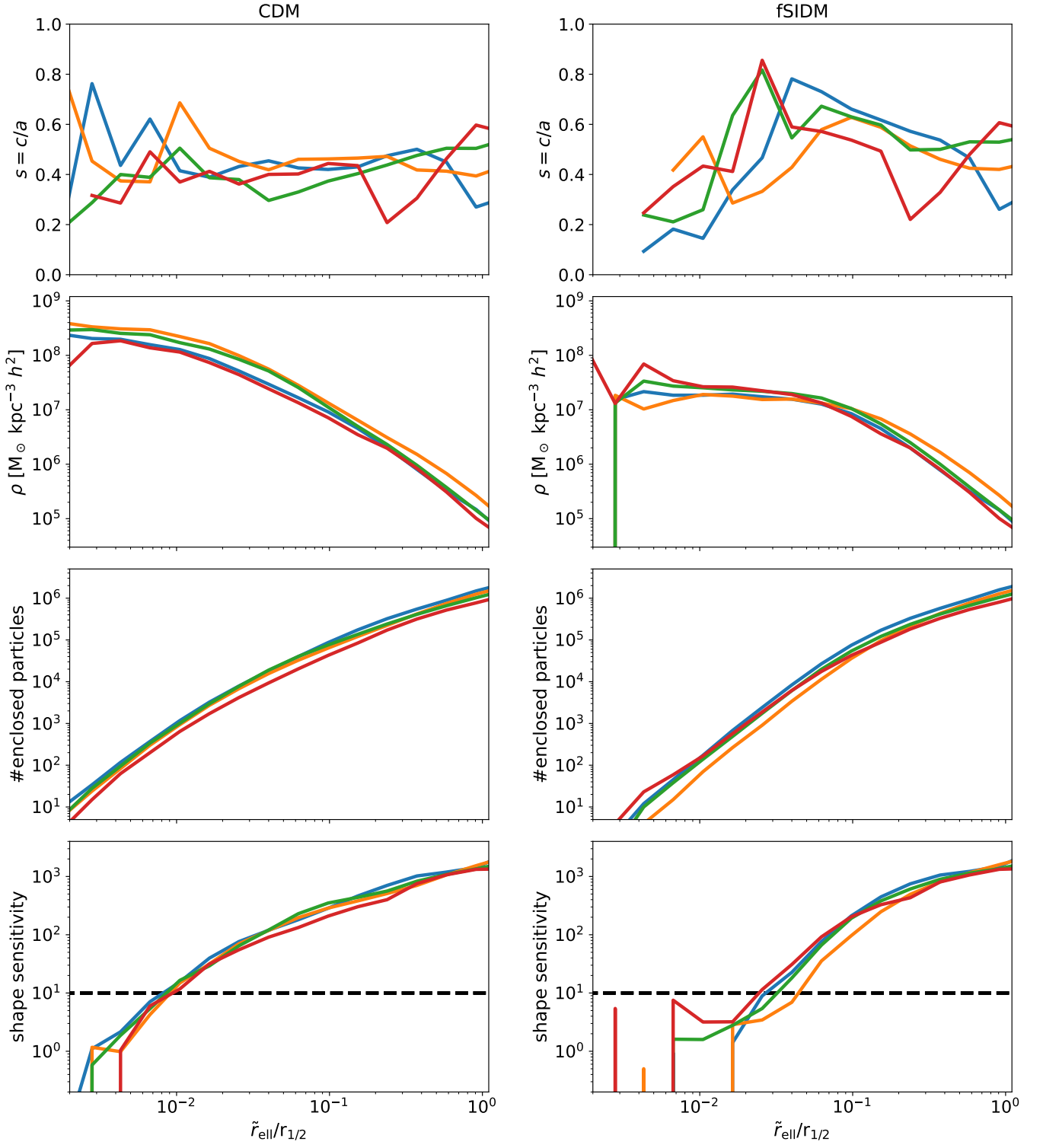


Fig. A.1. The same plot as in Fig. 2, but the shapes were computed using only particles within shells and not all particles enclosed in an ellipsoid. In consequence, Eq. 4 is used to compute the shape sensitivity.